Available online at www.sciencedirect.com
ScienceDirect
Carbohydrate Research 343 (2008) 132–138
Carbohydrate RESEARCH

Determining the solution conformational entropy of O-linked oligosaccharides at quasi-physiological conditions: size-exclusion chromatography and molecular dynamics

Marcus A. Boone,[a] Hugh Nymeyer[a,b] and André M. Striegel[a,*]

[a]*Department of Chemistry and Biochemistry, Florida State University, Tallahassee, FL 32306-3290, USA*
[b]*School of Computational Science, Florida State University, Tallahassee, FL 32306-3290, USA*

Received 14 April 2007; received in revised form 20 September 2007; accepted 26 September 2007
Available online 1 October 2007

Abstract—The physiological functions of oligosaccharides are influenced by a number of structural parameters such as anomeric configuration, glycosidic linkage, and degree of polymerization. These parameters affect the conformation of the oligosaccharides which, in turn, is responsible for characteristics such as aptameric and enzymatic binding, chiral recognition, and the structural targeting of bacterial and parasitic recognition events. Here, we measure the solution conformational entropy (ΔS) of two series of oligosaccharides, linear malto- and cellooligosaccharides, using size-exclusion chromatography (SEC). For each series, we have determined ΔS as a function of degree of polymerization (DP). The choice of oligosaccharides studied also allowed us to compare the influence of anomeric configuration on ΔS, and to do so as a function of DP. Studies were conducted in water at physiological temperature and pH in order to resemble conditions within the human body. Experimental results were augmented with results from molecular dynamics computer modeling simulations in aqueous solvent. A comparison between experimental and computational data showed how the techniques can complement each other. An example of the latter is the considerable enthalpic contribution to the chromatographic separation of α- and γ-cyclodextrin, which may have gone unnoticed if not for the large discrepancy between the results obtained by the separate techniques.

Keywords: Conformational entropy; Cellooligosaccharides; Maltooligosaccharides; Size-exclusion chromatography; Molecular dynamics; Quasi-physiological conditions

1. Introduction

Anomeric configuration, degree of polymerization, and their effect on solution conformation are integral factors in the fundamental roles oligosaccharides play in immune defense, fertilization, viral recognition, and cell growth and adhesion.[1] For malto- and cellooligosaccharides, which are used extensively in the food, feed, and pharmaceutical industries, degree of polymerization affects Michaelis constants,[2] turnover number,[2] chiral recognition,[3] and enzymatic binding,[4] while anomeric configuration influences properties such as cryptobiological cell protection[5] and enzymatic, bacterial, and aptameric docking and binding,[6–8] among others.

Estimates of the solution conformational entropy, ΔS, of oligosaccharides have traditionally been obtained through computer modeling.[9–14] While the modeling studies are usually performed in vacuo, most molecular recognition processes take place in solution. Recently, we began to explore the use of size-exclusion chromatography (SEC) for determining ΔS of mono-, di-, and oligosaccharides in solution and have been able to isolate the influences of a number of structural parameters on ΔS in select polar aprotic solvent systems.[15,16] These results, however, provide limited understanding of the conformational freedom of oligosaccharides in aqueous media, where most biological and physiological phenomena occur. To this end, the present set

* Corresponding author. Tel.: +1 850 645 3211; fax: +1 850 644 8281; e-mail: striegel@chem.fsu.edu

0008-6215/$ - see front matter © 2007 Elsevier Ltd. All rights reserved.
doi:10.1016/j.carres.2007.09.010

of experiments applies the methodology of SEC, an entropically driven separation method, to measuring the individual contributions of degree of polymerization and of anomeric configuration to the ΔS of linear malto- and cellooligosaccharides under conditions we term 'quasi-physiological'. This term is meant to imply the aqueous nature of the solvent, as well as temperature and pH conditions resembling those within the human body. The term does not include a polyelectrolytic component, due to the neutral nature of the oligosaccharides examined here.

We have augmented our experimental determination of ΔS with results from computer modeling studies under similar conditions. The purpose of this is twofold: Firstly, we intend to compare the experimental and computer modeling results to ascertain the degree of confidence that can be placed in the latter. Secondly, we intend to use the modeling results to guide our understanding of the separation process. While large discrepancies between modeling and experimental results may be due to the level of approximation of the model, they may also be due to non-size-exclusion effects in the separation process (or due to both), which may lead to a re-examination of the experimental data.

The particular oligosaccharides examined here are the series maltose through maltoheptaose and cellobiose through cellopentaose. We also studied the cyclic analogs of maltohexaose and maltooctaose, namely, α- and γ-cyclodextrin. It is in the study of these cyclodextrins that results from computer modeling using molecular dynamics (MD) simulations proved most informative of the non-size-exclusion effects contributing to the chromatographic separation of the cyclic oligomers. We believe that the results of these studies provide valuable conclusions for those working in areas such as glycopharmaceuticals, plant polymers, and biomolecular recognition and mimicry, provide experimental data for those working in the area of computer modeling, and will help expand our understanding of the fundamental separation processes involved in the determination of ΔS.

2. Results and discussion

Results from our SEC experiments, carried out under aqueous, quasi-physiological conditions of temperature and pH, are shown in Table 1 and Figure 1. Also shown are results of the molecular dynamics simulations of the same oligosaccharides, carried out in explicit aqueous solvent as described in Section 3. These results differ from previous results in neat *N*,*N*-dimethylacetamide (DMAc) and in DMAc/LiCl due to differences in pore sizes between the SEC columns used in the present experiments and the columns used in the organic solvent experiments. Also, the $-\Delta S$ values reflect the solution conformational entropy of the solvated oligomers; in the present experiments, the oligosaccharides are solvated by several water molecules, while in previous experiments solvation was either by several DMAc molecules or by several macrocations of the form $[DMAc_n+Li]^+$, both of which are substantially bulkier than a molecule of H_2O.[17] Maltooligosaccharides (M series) are linear α-(1→4)-linked oligomers, whereas

Table 1. $-\Delta S$ of oligosaccharides in H_2O (37 °C, pH 7.39) as determined by size-exclusion chromatography (SEC) and molecular dynamics

Oligosaccharide	$-\Delta S$ (SEC) (J mol^{-1} K^{-1})	$-\Delta S$ (molecular dynamics) (J mol^{-1} K^{-1})
α-D-Glucose (M_1)	2.002 ± 0.003	2.50 ± 0.01
Maltose (M_2)	3.266 ± 0.006	3.45 ± 0.01
Maltotriose (M_3)	4.362 ± 0.001	4.35 ± 0.02
Maltotetraose (M_4)	5.295 ± 0.003	5.11 ± 0.02
Maltopentaose (M_5)	6.063 ± 0.000	5.99 ± 0.03
Maltohexaose (M_6)	6.725 ± 0.004	6.61 ± 0.04
Maltoheptaose (M_7)	7.308 ± 0.002	7.77 ± 0.05
Cellobiose (C_2)	3.603 ± 0.004	3.54 ± 0.01
Cellotriose (C_3)	5.006 ± 0.002	4.67 ± 0.01
Cellotetraose (C_4)	6.185 ± 0.007	5.88 ± 0.02
Cellopentaose (C_5)	7.229 ± 0.001	7.25 ± 0.02
α-Cyclodextrin (α-CD)	(2.302 ± 0.001)[a]	5.90 ± 0.50
γ-Cyclodextrin (γ-CD)	(3.621 ± 0.005)[a]	7.20 ± 0.50

[a] CD data using SEC are reported here only for comparison to molecular dynamics results. SEC analysis of the CDs did not occur by a strict size-exclusion mechanism, but, instead, reflects a substantial enthalpic contribution to the separation. See text for discussion.

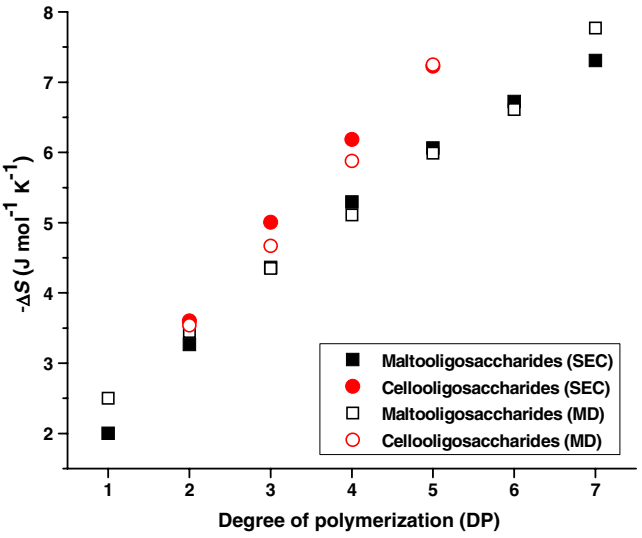

Figure 1. Solution conformational entropy ($-\Delta S$) of linear malto- and cellooligosaccharides as a function of degree of polymerization (DP). Circles correspond to cellooligosaccharides, squares to maltooligosaccharides. Filled symbols represent experimental SEC results, open symbols denote molecular dynamics (MD) results. All were data obtained in H_2O at 37 °C, pH 7.39. In all cases, standard deviation is substantially smaller than data markers and, therefore, not shown.

the linkage in the cellooligosaccharides (C series), which are also linear, is β-(1→4). For this set of experiments we used maltooligosaccharides with degree of polymerization (DP) 1–7 (M_1–M_7) and cellooligosaccharides with DP 2–5 (C_2–C_5). We proceed to discuss the individual effects of DP and anomeric configuration on $-\Delta S$ and to compare experimental and computational results. Regarding the latter comparison, we also examine results obtained for several cyclomaltooligosaccharides (cyclodextrins).

The conformational space occupied by a polymer or an oligomer increases with each added monomer unit.[18] For the oligosaccharides studied, this is reflected in a monotonic increase in $-\Delta S$ with increasing DP, as seen in Table 1 and Figure 1. This relationship extends to the hydrodynamic volume occupied by the oligosaccharides in solution, with hydrodynamic volume governing elution order in SEC (analytes occupying a larger hydrodynamic volume in solution elute earlier than those occupying a smaller volume). Evidence of this is given in Figure 2, in which the pentamers of each series are observed to elute earlier in an SEC experiment, and are separated with near-baseline resolution, from tetramers of the same series. The steady increase in $-\Delta S$ with DP is also seen in our computer modeling results, where simulation trends mimic experimental data. It is worth noting that the $\Delta\Delta S$ between M_2 and M_7 (4.042 J mol^{-1} K^{-1}), between M_2 and M_5 (2.797 J mol^{-1} K^{-1}), and between C_2 and C_5 (3.626 J mol^{-1} K^{-1}) derived from the experimental data are closely matched by the $\Delta\Delta S$ obtained from the molecular dynamics simulations.

Comparing conformational isomers of the same DP, we find that the β anomers have consistently higher $-\Delta S$ than their α counterparts, attributed primarily to the greater flexibility of the equatorial glycosidic bond in the former as compared to the corresponding axial bond in the latter (given identical glycosidic linkages),[19] and also to the reported preference of the hydroxyl groups in β-D-glucopyranoses to reorient themselves upon interaction with water molecules, as compared to the hydroxyl groups in α-D-glucopyranoses.[13] When comparing the series dimer through pentamer we notice that as DP increases, so does the $\Delta\Delta S$ between anomers. Another way of stating this is to say that there is a faster change in $-\Delta S$ as a function of DP for the cello series than for the malto series. This result, which is closely matched by the computer modeling calculations, is attributed to the strong energy minima in the O1–C1–O4′–C4′ and in the C1–O4′–C4′–C5′ torsion angles of the repeat unit of the maltooligosaccharides.[20] Continued addition of repeat units in the malto series ultimately produces one strand of the amylose double helix.

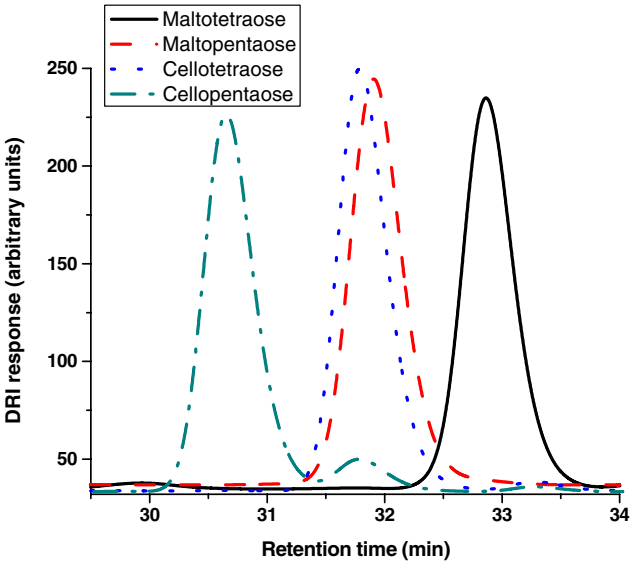

Figure 2. SEC/DRI elution profiles of maltotetraose, maltopentaose, cellotetraose, and cellopentaose (H_2O, 37 °C, pH 7.39).

As mentioned, computer modeling was found to adequately simulate important trends such as the higher solution conformational entropy of the cellooligosaccharides as compared to linear maltooligosaccharides of the same DP, as well as to adequately simulate the increase in $-\Delta S$ with increasing DP for each series. The molecular dynamics results for all the data have one adjustable parameter: The cavity diameter of pores in the SEC matrix. Pores in the SEC matrix were assumed to be spherical with a diameter D. A global fit to all the malto- and cellooligosaccharide data suggested a value of $D = 78$ Å, which is the value used in all the calculations. This is 35% smaller than the manufacturer's reported diameter of 120 Å, determined from measurements of the exclusion limit of the column. This discrepancy may be a compensation for deficiencies of the simulations; alternatively, this value may accurately reflect the polydispersity in size and shape of the pores in the SEC column.

A brief discussion may help to clarify the role of pore geometry on the best-fit value of D. As shown by Giddings et al.,[21] the partition function K_{SEC} for ideal size-exclusion separation of molecules with fixed geometry has the form

$$K_{SEC} = \left(1 - \frac{r_{molecule}}{r_{cavity}}\right)^m$$

where $r_{molecule}$ and r_{cavity} are characteristic dimensions of the molecule and cavity, respectively, and m is a parameter characteristic of the geometry. For spherical particles in slit-shaped pores, cylindrical pores, and spherical pores m takes on values of 1, 2, and 3, respectively. For pores in which $r_{molecule}$ is much smaller than r_{cavity},

$$K_{SEC} \approx 1 - m\frac{r_{molecule}}{r_{cavity}}$$

and

$$\Delta S = -R \ln K_{SEC} \approx mR \frac{r_{molecule}}{r_{cavity}}$$

In particular, if the cavity is relatively elongated, then its longest dimension—which will largely determine the exclusion size of the cavity—may be significantly greater than its shorter dimension, r_{cavity}, which controls ΔS. Cavity asymmetry is thus a plausible reason for the discrepancy between the value of D from fitting and that provided by the manufacturer. Alternatively, irregularly shaped cavity walls on the scale of a single sugar molecule would result in an increased surface area-to-volume ratio. Following the analysis of Giddings et al.,[21] this alteration would be expected to increase the value of ΔS and consequently decrease the apparent value of r_{cavity}.

Regardless of the origin of the apparent cavity radius, analysis of the computational data with a value of D near 120 Å results in values of $-\Delta S$ that are much too small even for the smallest oligosaccharides (maltose and cellobiose). The large discrepancy in these oligosaccharides is difficult to rationalize as a defect in the force field or in the amount of sampling.

Of course, any asymmetry in pore shape would also affect the dependence of $-\Delta S$ on DP. For elongated molecules like the oligosaccharides studied here, elongated cavities would manifest themselves as additional downward curvature in the dependence of $-\Delta S$ on DP. This type of discrepancy is observed: Computational results indicate that $-\Delta S$ is nearly linear with respect to DP, but experimentally there is a downward curvature in $-\Delta S$ as DP is increased (see Fig. 1).

Although additional parameters could be introduced to model pore size polydispersity and pore asymmetry in the SEC columns, this would necessitate the introduction of additional parameters to be fit, which we did not feel was warranted considering the number of independent data points. Analysis of the molecular dynamics data assuming asymmetric cavities of different size did indicate, however, that the choice of D and the amount of asymmetry had only a weak effect on the differences between malto- and cellooligosaccharide values for the same DP.

One area where the experiment was able to show some limitation of the computational method was in the relationship between the $\Delta\Delta S$ of anomer pairs and DP. As seen in Table 2 for the range dimer through pentamer, $\Delta\Delta S$ as determined from SEC results varied linearly with DP, whereas $\Delta\Delta S$ from molecular dynamics simulations increased exponentially with DP. As a result of these different rates of change, the $\Delta\Delta S$ of the lower DP anomer pairs is underestimated by computer modeling while the $\Delta\Delta S$ of the highest anomer pair studied is slightly overestimated. Further experiments are planned in this regard, using different cavity sizes as well as different cavity shapes.

Table 2. $\Delta\Delta S$ for anomer pairs, by SEC and MD

Anomer pair	$\Delta\Delta S$ (SEC) (J mol^{-1} K^{-1})	$\Delta\Delta S$ (MD) (J mol^{-1} K^{-1})
M_2–C_2	0.337	0.09
M_3–C_3	0.644	0.32
M_4–C_4	0.890	0.77
M_5–C_5	1.166	1.26

The cooperative nature of the relationship between experiment and simulation was again demonstrated when studying cyclomaltooligosaccharides (cyclodextrins, CDs). Firstly, we note that we were only able to study α-CD and γ-CD, the cyclic equivalents of maltohexaose and maltooctaose, respectively, as the seven-membered ring β-CD (the cyclic equivalent of maltoheptaose) was found to be insoluble in our aqueous medium. Indeed, studies have shown β-CD to be at least nine times less soluble in water than α-CD and eleven times less soluble than γ-CD.[22] Interestingly, these solubility differences are attributed to an entropic effect, as the enthalpies of solution of the three CDs are quite similar to each other. Also tangentially related to the present study, it was molecular dynamics that revealed that β-CD induces a stronger ordering on the surrounding water molecules than do the other two cyclodextrins, lowering the conformational entropy that purportedly causes the seemingly abnormal solubility of β-CD.[23]

Secondly, we note that a large discrepancy was observed between our MD and SEC results for $-\Delta S$ of α-and γ-CD, as seen in Table 1. We had originally checked that our SEC experiments were being conducted at 'near-ideal' SEC conditions, that is, in the virtual absence of enthalpic effects, by examining the highest and the lowest homologs of each linear series at two different temperatures, 25 and 37 °C. As seen in Table 3, a difference of less than 3 parts per hundred was observed between the K_{SEC} of maltose, maltoheptaose, cellobiose, and cellopentaose when measured at the two different temperatures, confirming that chromatographic elution was almost exclusively controlled by entropic factors. We had assumed that the CDs were also eluting by a strict size-exclusion mechanism and had not checked for a temperature dependence of their distribution coefficients. Guided by the MD results, we

Table 3. Solute distribution coefficient (K_{SEC}) as a function of temperature

Oligosaccharide	K_{SEC} (25 °C)	K_{SEC} (37 °C)
Maltose (M_2)	0.683	0.675
Maltoheptaose (M_7)	0.430	0.415
Cellobiose (C_2)	0.657	0.648
Cellopentaose (C_5)	0.431	0.419
α-Cyclodextrin (α-CD)	0.890	0.758
γ-Cyclodextrin (γ-CD)	0.718	0.647

performed this check. As seen in Table 3, the elution of α- and γ-CD is driven by a substantial enthalpic component, as evidenced by the large change, on the order of 10–15%, between the K_{SEC} values determined at 25 versus 37 °C. We thus see how computer simulation has the ability to inform our knowledge of the separation processes and to point us in the direction of possible errors.

3. Experimental

3.1. Materials

Oligosaccharides and glucose were purchased from Sigma–Aldrich. All carbohydrates are of the D-series and sold to at least 95% purity by the manufacturer. Carbohydrates were used as received, without further purification. Acetone was purchased from Fisher Chemical Co., MeOH and NaOH from VWR Scientific Co., and pullulan standard from Polymer Laboratories.

3.2. Size-exclusion chromatography (SEC)

Unfiltered sample injections (injection volume = 100 μL, concentration = 2.5 mg/mL in H_2O) were analyzed with an SEC system using degassed, deionized H_2O as mobile phase at 1.000 mL/min flow rate. Eluent temperature was 37 °C, with pH adjusted to 7.39 using 1 M NaOH. Separation occurred over a column bank consisting of four analytical Ultrahyrogel 6-μm particle size, 120 Å pore size SEC columns, purchased from Waters Corp. Detection was performed with a Waters 410 differential refractive index (DRI) detector. Column, detector, and injection compartment temperatures were maintained at 37.0 ± 0.1 °C. The interconnecting tubing between the column bank and the detector was wrapped with insulating tape to prevent heat loss during transfer. For all chromatographic determinations, results are the averages of six injections, three each from two separate sample solution vials. Minor flow rate fluctuations for the saccharide measurements were corrected by comparing the retention time of an acetone marker peak in each injection (including individual maltose injections) to the average value of this peak for all maltose injections. Data acquisition was performed using Clarity software (V. 2.4.0.195) from Data Apex.

3.3. Calculation of $-\Delta S$ of oligosaccharides[24,25]

Calculation of the standard conformational entropy difference between mobile and stationary phases for the oligosaccharides in solution was based on the retention times of the peak maxima (V_R), as measured by SEC, as well as on the solute distribution coefficients (K_{SEC}). These two parameters are related via

$$K_{SEC} = \frac{V_R - V_0}{V_i - V_0}$$

where V_0 is the void volume of the columns and V_i is the total column volume. The internal pore volume of the system is defined as the difference between V_i and V_0. The SEC columns are quoted by the manufacturer as having an exclusion limit of approximately 5000 g/mol, based on the analysis of poly(ethylene oxide) and poly(ethylene glycol) standards in water. We measured V_0 using a 22,800 g/mol narrow polydispersity ($M_w/M_n = 1.07$) pullulan standard, and measured V_i using acetone. As seen in Table 3, for the linear oligosaccharides we observe a difference of three parts per hundred or less in the values of K_{SEC} for maltose, maltoheptaose, cellobiose, and cellopentaose when measured at 25 versus at 37 °C. This strongly supports the conclusion that separation of the linear malto- and cellooligosaccharides is predominantly entropic in nature (characteristic of 'near-ideal' SEC behavior), as enthalpic interactions with the column packing material would lead to highly temperature-dependent values of the distribution coefficient (as observed with the cyclodextrins; see Table 3). Consequently, we can write

$$\Delta S = R \ln K_{SEC}$$

Here, we have used $R = 8.31451\ \mathrm{J\ mol^{-1}\ K^{-1}}$. The standard entropy difference, $-\Delta S$, denotes the difference between the conformational entropy of the oligosaccharides in the flowing mobile phase outside the pores of the column packing and the entropy of the oligosaccharides in the stagnant mobile phase inside the pores. The use of the negative sign (i.e., of $-\Delta S$) is a result of solute permeation in SEC being associated with a decrease in conformational entropy due to the more limited analyte mobility inside the pores as compared to analyte mobility in the interstitial volume.

3.4. Simulation techniques

Simulations of the malto- and cellooligosaccharides and cyclodextrins were performed using the AMBER suite of molecular dynamics programs (version 8).[26] The GLYCAM-04 force field was used for all simulations.[26,27] The carbohydrate topology and initial coordinates were constructed using the program LEAP.[26] All carbohydrates were solvated using TIP3P waters.[28] The simulations were done using periodic boundary conditions at constant temperature. All systems were minimized, equilibrated for a minimum of 1 ns, and followed by a production run of 10 ns. Equilibration was performed in an NpT ensemble at 1 atm and 37 °C. Production runs were either NVT (malto and cello series) using the final equilibrated volume or NpT (cyclodextrins). A timestep of 2 fs was used, and samples were taken at 0.5 ps intervals. SHAKE/RATTLE[29,30] was used to

constrain all bonds involving hydrogen, and SETTLE[31] was used to maintain a rigid water model. Temperature and pressure were maintained via a weak coupling algorithm,[32] with coupling times of 1 ps. Electrostatic interactions were calculated using the Particle–Mesh–Ewald method,[33] with a 4th-order Lagrange interpolation for the charges, a grid spacing no larger than 1 Å, and a screening charge width of approximately 2.5 Å. Tin-foil boundary conditions were maintained at infinity. Short-range interactions were switched off smoothly starting at 8 Å, and a tail correction was applied for the electrostatic and Leonard–Jones interactions. Linear center of mass motion was periodically removed. Pair-list updates were performed every 10 integration steps. No scaling was applied for 1–4 interactions to be consistent with the GLYCAM-04 force field.

Following Giddings et al.,[21] $-\Delta S$ was computed by assuming that the carbohydrates are sterically restricted when in the stationary phase. $-\Delta S$ was computed as $\Delta S = R\ln f$, where f is the fraction of volume that is accessible to the carbohydrate. The accessible volume f is taken as the fraction of sites for which all carbohydrate atoms are no closer than 1 Å from the walls of the stationary-phase cavities. Accessible volume was determined by a grid search using a 1 Å grid. The error induced by using a 1 Å grid was tested on selected sets of data and found to be less than sampling errors in all cases. Stationary-phase cavities are assumed to be spherical with a uniform diameter D, which was globally fit to the malto- and cellooligosaccharide data. The exact shape and size distribution of the cavities is unknown, and our choice appears to be a reasonable choice considering our data and existing analyses of SEC cavity dimensions. All results presented here were made with $D = 78$ Å. Approximate error bars are determined by block averages.

The method we use to determine $-\Delta S$ from the simulations is a rigorous application of free-energy perturbation, albeit one which makes minimal assumptions about the nature of the actual interactions between the cavity walls and oligosaccharides. Starting from the standard free-energy perturbation expression, we can determine the free-energy change created by the introduction of cavity walls as

$$\begin{aligned}\Delta G &= -RT\ln\left\langle e^{-\Delta H/RT}\right\rangle_0 \\ &= -RT\ln(fe^{-0/RT} + (1-f)e^{-\infty/RT}) = -RT\ln f\end{aligned}$$

where subscript 0 indicates a thermal average over the saccharide simulated without cavity walls and ΔH is the change in enthalpy upon the introduction of the cavity walls. The primary assumption is that the cavity has no effect upon the oligosaccharide conformation when it is not in contact with the cavity walls ($\Delta H = 0$). Recent simulations suggest that small hydrophobic cavities may have significantly altered water structure near their surface, which may affect the oligosaccharide structure in other ways.[34] In addition, we assume that the change in free energy of the saccharide is unchanged when not in a cavity. This is equivalent to assuming that the relative surface area-to-volume ratio is negligible outside of the cavities of the SEC column.

The simple assumption about the type of cavity–oligosaccharide interactions is supported by the SEC data, which show a minimal contribution of ΔH to K_{SEC}. Also, it is convenient, because it does not require any additional knowledge or assumptions about the atomic- and nano-scale structure of the pores. Although additional information about the pore structure would allow for more detailed perturbative calculations, these calculations would be at the limit of existing computational means and would introduce additional computational uncertainty.

4. Conclusions

Size-exclusion chromatography was used to determine the solution conformational entropy of two series of linear O-linked oligosaccharides, maltooligosaccharides and cellooligosaccharides, in water at quasi-physiological conditions of temperature and pH. For each series $-\Delta S$ was observed to increase steadily with degree of polymerization, though a faster rate of increase was displayed by the cellooligosaccharides over their malto counterparts. Comparison between members of each series with the same DP confirmed the larger conformational freedom (higher flexibility) afforded by the equatorial β anomeric configuration as compared to the axial α anomeric configuration, given the same (1→4)-type glycosidic linkage and the same D-anhydroglucose constituent monosaccharide units. Comparison between linear and cyclic α-(1→4)-linked oligosaccharides was precluded by the extremely low solubility of β-cyclodextrin as well as by the large enthalpic contribution to the SEC analysis of α- and γ-cyclodextrin.

Experimental SEC results were augmented by those obtained using molecular dynamics computer modeling simulations. In most cases, the latter modeled trends in the experimental data quite well and even quantitative comparisons between experimental and simulation-generated data sets were possible. An exception was the case of the $\Delta\Delta S$ between anomer pairs where, over the DP range 2–5, the experimentally determined $\Delta\Delta S$ grew linearly with DP, whereas the $\Delta\Delta S$ derived from simulation data grew exponentially with DP. As a result of this, the $\Delta\Delta S$ between anomers of DP 2–4 was underestimated by computer modeling, whereas the $\Delta\Delta S$ between DP 5 anomers was overestimated by the simulations. It is important, however, to also point out that the first indication that α- and γ-cyclodextrin did not elute via a strict size-exclusion mechanism was provided

by the computer modeling simulations. This behavior of the cyclodextrins was subsequently confirmed experimentally.

The experimental approach and results presented here can contribute to our growing understanding of the influence of structural parameters such as anomeric configuration, glycosidic linkage, degree of polymerization, etc. on the solution behavior of carbohydrates and on their physiological roles. This understanding is augmented by the insights provided by computer modeling, which appears to adequately represent the experimental data and which also provides insight regarding potential experimental pitfalls.

References

1. Osborn, H.; Khan, T. *Oligosaccharides—Their Synthesis and Biological Roles*; Oxford: New York, 2000.
2. Nitta, Y.; Mizushima, M.; Hiromi, K.; Ono, S. *J. Biochem.* **1971**, *69*, 567–576.
3. Chankvetadze, B.; Saito, M.; Yashima, E.; Okamoto, Y. *Chirality* **1998**, *10*, 134–139.
4. Johnson, P. E.; Tomme, P.; Joshi, M. D.; McIntosh, L. P. *Biochemistry* **1996**, *35*, 13895–13906.
5. Magazù, S.; Villari, V.; Faraone, A.; Maisano, G.; Heenan, R. K.; King, S. *J. Phys. Chem. B* **2002**, *106*, 6954–6960.
6. Lindberg, A. A.; Brown, J. E.; Strömberg, N.; Westling-Ryd, M.; Schultz, J. E.; Karlsson, K.-A. *J. Biol. Chem.* **1987**, *262*, 1779–1785.
7. Rockey, W. M.; Laederach, A.; Reilly, P. J. *Proteins* **2000**, *40*, 299–309.
8. Yang, Q.; Goldstein, I. J.; Mei, H.-Y.; Engelke, D. R. *Proc. Natl. Acad. Sci. U.S.A.* **1998**, *95*, 5462–5467.
9. Momany, F. A.; Willett, J. L. *J. Comput. Chem.* **2000**, *21*, 1204–1219.
10. Brady, J. W.; Schmidt, R. K. *J. Phys. Chem.* **1993**, *97*, 958–966.
11. Schmidt, R. K.; Teo, B.; Brady, J. W. *J. Phys. Chem.* **1995**, *99*, 11339–11343.
12. Chen, J.; Naidoo, K. *J. Phys. Chem. B* **2003**, *107*, 9558–9566.
13. Momany, F. A.; Appell, M.; Strati, G.; Willett, J. L. *Carbohydr. Res.* **2004**, *339*, 553–567.
14. Corchado, J. C.; Aguilar, M. A. *J. Am. Chem. Soc.* **2004**, *126*, 7311–7319.
15. Striegel, A. M. *J. Am. Chem. Soc.* **2003**, *125*, 4146–4148 (see Erratum in Striegel, A.M. *J. Am. Chem. Soc*. **2004**, *126*, 4740).
16. Boone, M. A.; Striegel, A. M. *Macromolecules* **2006**, *39*, 4128–4131.
17. Striegel, A. M. *J. Chilean Chem. Soc.* **2003**, *48*, 73–78.
18. Stoddart, J. F. *Stereochemistry of Carbohydrates*; Wiley: New York, 1971.
19. Rees, D. A.; Morris, E. R.; Thom, D.; Madden, J. K. In *The Polysaccharides*; Aspinall, G. O., Ed.; Academic Press: New York, 1982; Vol. 1, pp 195–290.
20. Hancock, R. D.; Tarbet, B. J. *J. Chem. Educ.* **2000**, *77*, 988–992.
21. Giddings, J. C.; Kucera, E.; Russell, C. P.; Myers, M. N. *J. Phys. Chem.* **1968**, *72*, 4397–4408.
22. Sabadini, E.; Cosgrove, T.; Egídio, F. C. *Carbohydr. Res.* **2006**, *341*, 270–274.
23. Naidoo, K. J.; Chen, J. Y.; Jansson, J. L. M.; Widmalm, G.; Maliniak, A. *J. Phys. Chem. B* **2004**, *108*, 4236–4238.
24. Striegel, A. M. *J. Chromatogr. A* **2004**, *1033*, 241–245.
25. Yau, W. W.; Kirkland, J. J.; Bly, D. D. *Modern Size-Exclusion Liquid Chromatography*; Wiley: New York, 1979.
26. Case, D. A.; Cheatham, T. E., III.; Darden, T.; Gohlke, H.; Luo, R.; Merz, K. M., Jr.; Onufriev, A.; Simmerling, C.; Wang, B.; Woods, R. J. *J. Comput. Chem.* **2005**, *26*, 1668–1688.
27. Woods Group. *GLYCAM Web*. 2006 [cited 1 March 2006]; Available from: http://www.glycam.com.
28. Jorgensen, W. L.; Chandrasekhar, J.; Madura, J. D.; Impey, R. W.; Klein, M. L. *J. Chem. Phys.* **1983**, *79*, 926–935.
29. Yoneya, M.; Berendsen, H. J. C.; Hirasawa, K. *Mol. Simul.* **1994**, *13*, 395–405.
30. Ryckaert, J.-P.; Ciccotti, G.; Berendsen, H. J. C. *J. Comput. Phys.* **1977**, *23*, 327–341.
31. Miyamoto, S.; Kollman, P. A. *J. Comput. Chem.* **1992**, *13*, 952–962.
32. Berendsen, H. J. C.; Postma, J. P. M.; van Gusteren, W. F.; DiNola, A.; Haak, J. R. *J. Chem. Phys.* **1984**, *81*, 3584–3590.
33. Darden, T.; York, D.; Pedersen, L. *J. Chem. Phys.* **1993**, *98*, 10089–10092.
34. Lucent, D.; Vishal, V.; Pande, V. S. *Proc. Natl. Acad. Sci. U.S.A.* **2007**, *104*, 10430–10434.